DUPLICATE ALSO

HADLEY CENTRE
FOR CLIMATE PREDICTION AND RESEARCH

The simulation of the tropical oceans in models of different horizontal resolution

by

C Gordon, D K Wright and C M Roberts

CRTN 58

May 1995

CLIMATE
RESEARCH
TECHNICAL
NOTE

Hadley Centre
Meteorological Office
London Road
Bracknell
Berkshire RG12 2SY

FHSC
National Mete
London Rd, Brack
ORGS UKMO C
National Meteorological Library
FitzRoy Road, Exeter, Devon. EX1 3PB

CLIMATE RESEARCH TECHNICAL NOTE NO. 58

THE SIMULATION OF THE TROPICAL OCEANS IN MODELS OF DIFFERENT HORIZONTAL RESOLUTION

by

C Gordon, D K Wright and C M Roberts

Hadley Centre for Climate Prediction and Research
Meteorological Office
London Road
Bracknell
Berkshire RG12 2SY

NOTE: This paper has not been published. Permission to quote from it should be obtained from the Director of the Hadley Centre.

1. Introduction

The ability of models to simulate the tropical Pacific ocean is of particular importance for a number of reasons. Firstly, in common with the other tropical oceans, there is a richness of ocean current structure with features such as the Equatorial Under-Current (EUC), the South Equatorial Current (SEC), North Equatorial Current (NEC) and the North Equatorial Counter Current (NECC) which makes the tropics an excellent test bed for models. In addition to this variety of mean current structures, a transient phenomena unique to the Pacific is the El Nino which is the largest climate signal on the interannual timescale.

It is of particular interest to consider how the El Nino Southern Oscillation (ENSO) will alter in a scenario of global man made climate change (Meehl et al, 1993, Knutson and Manabe, 1994 and Tett, 1995) since any alteration in ENSO could produce very large local climate variations and have implications for teleconnections to higher latitudes. The study of ENSO over the last decade has led to a number of proposed mechanisms for the production of the ENSO cycle and when considering climate model studies into changes in this cycle it is important to consider how well the models concerned represent these mechanisms.

A variety of studies have been carried out in recent years to investigate the ENSO phenomena in general circulation models of the ocean-atmosphere climate system. Philander et al (1989) considered the simulation of ENSO in two coupled models with the same atmospheric component but with a global low (in the horizontal and vertical) resolution ocean model and with a high resolution tropical Pacific ocean model. The mechanisms for ENSO are quite different in each of the models which Philander et al (1993) attribute to the lack of resolution in the coarse ocean version.

Knutson and Manabe (1994) in their study of ENSO behaviour in a coupled model with a coarse ocean resolution (4.5°x3.75° latitude-longitude) point out that the variability they see in their simulations has 50% of the amplitude of that found in an equivalent model with a high resolution ocean component. They also point out that in their low resolution model El Nino tends to be characterised by an 'SST mode' (Neelin, 1991 - see later) and that the model under-emphasises the role of the subsurface ocean dynamics when compared to the higher resolution models.

Tett (1994) used a coupled model with the ocean component identical to the 2.5°x3.75° coarse resolution model described later in this note. He identified two major mechanisms for the ENSO-like oscillations in his model which are probably associated with local coupled SST modes (Tett, private communication).

Our purpose in this note is to quantify the effects of meridional resolution in a general circulation ocean model on the simulated dynamics associated with the tropical oceans.

Most of the work carried out to simulate the ENSO cycle has involved either simplified ocean models or high resolution, usually of order 1/3 - 1/2° in the meridional direction, simulations with ocean general circulation models (Mechoso et al, 1995). The reason for the high meridional resolution is that the north-south scale of dynamical features in the equatorial oceans, both of the mean and transient, is set by the equatorial Rossby radius of deformation:

$$a_e=(c/2\beta)^{1/2} \qquad (1)$$

where c is the internal gravity wave speed for a given ocean mode, and β is the north south derivative of the Coriolis parameter evaluated at the equator (See Gill, 1982 for details). For the tropical oceans typical baroclinic phase speeds are 0.5 - 3 ms^{-1}, which gives an equatorial Rossby radius of 100-250 km (or 1° to 2.5° of longitude). The 1/3° - 1/2° meridional model resolution mentioned above is needed to resolve the mean and transient ocean features that occur with a scale determined by the Rossby radius.

In climate change experiments it is necessary to integrate the coupled models for long periods of time to bring the coupled system some way towards equilibrium. For this reason the integrations are expensive to perform and coarse resolution ocean models are usually employed. At the Hadley Centre a horizontal resolution of 2.5°x3.75° latitude-longitude has been used extensively which is a relatively high ocean model resolution for this type of experiment. Now clearly, at this resolution, there is no possibility of resolving the equatorial Rossby radius and therefore the mean and transient features referred to above. So the question arises as to how well these models represent the tropical oceans? As noted above, despite their coarse resolution it is also fairly well

documented that these models do produce an 'ENSO-like cycle' although the mechanisms may be different to those in the higher resolution models and to those in reality.

In this paper we consider three different ocean simulations of the tropical Pacific with meridional resolution from 1/3° to 2.5° on the equator. The purpose is to compare the simulations with each other, and with reality where possible, and attempt to further understand the processes at play in each of the models. We will consider both the mean simulation and transient features.

Section 2 describes the models, their initialisation and the forcing used. Sections 3 and 4 consider the simulation of the mean and transient features respectively. Section 5 looks at the implications for ENSO mechanisms in the models and, finally, in Section 6 some conclusions are drawn and the implications for coupled models discussed.

2. The Models, Forcing and Initial Conditions

Three different versions of the Cox (1984) model were used in the intercomparison described in this paper. The 'control' simulation was performed with a high resolution model of the tropical Pacific ocean between 30°N and 30°S. The model has 16 levels in the vertical with a flat bottom at 4000m. The vertical levels are distributed so as to give maximum resolution in the mixed layer and near the ocean surface the first five levels have a spacing of around 10m. The horizontal grid is irregular with a meridional resolution of 1/3° near the equator decreasing to 1° at 30°N and 30°S. In the east-west direction the resolution is also variable with a grid spacing of 1.5° in the central Pacific decreasing to about ½° at the eastern and western boundaries. This is a baroclinic model in that the barotropic part is set to zero throughout. This is a reasonable approximation for the upper tropical oceans where the baroclinic part dominates the flow. This model is regarded as the control because it has already been established that it is well capable of resolving the tropical features of interest. Further details of this model can be found in Gordon and Corry (1991).

The second model is the global coarse resolution ocean model that has been used at the Hadley Centre for climate change integrations (Murphy, 1995). It

has 20 vertical levels with a distribution identical to that in the tropical model in the upper 1000m. Below that level the distribution of levels differ. The global model also includes the variations in ocean bottom topography. It also includes the barotropic part and has a uniform 2.5°x3.75° latitude-longitude grid.

The final model is also global in extent and has the same vertical distribution of levels as the coarse global model. It has a uniform 1°x1° latitude-longitude grid with variable bottom topography and again explicitly includes the barotropic part.

All of the models have the same representation of vertical mixing near the ocean surface. In each case there is the same embedded Kraus-Turner mixed layer model and, in addition, a Richardson number dependent vertical diffusion. The parameters in these schemes are the same in each of the above models. The horizontal diffusion is a simple Laplacian term in the momentum equations and the eddy viscosity is chosen in order to maintain numerical stability and is also a function of the local grid spacing. The value at the equator in the 2.5°x3.75° model is $3x10^9 cm^2 s^{-1}$, in the 1°x1° model it is $6x10^7 cm^2 s^{-1}$ and in the tropical Pacific model $2x10^7 cm^2 s^{-1}$. A physically reasonable value is thought to be $O(10^7)$ and the high value in the coarse resolution model is necessary to maintain numerical stability. Clearly this large momentum diffusion will also have a significant effect on the relatively small scale tropical features. The tracer diffusion in the high resolution tropical model has a constant value of $2x10^7 cm^2 s^{-1}$. In the global models the scheme of Redi (1982) is used in which mixing is predominantly along isopycnal surfaces. Table 1 summarises the characteristics of each of the models.

MODEL	RESOLUTION	HORIZONTAL EDDY VISCOSITY (cm^2s^{-1})
Tropical Pacific 30°N to 30°S	1/3° on the equator changing to 1° at ±30°. 1/2° at the eastern and western coasts changing to 1.5° in the central Pacific. 16 Levels with 8 levels in the upper 200m. Horizontal tracer diffusion.	$2x10^7x(\Delta/1/3°)$ cm^2s^{-1} (Δ=local grid spacing)
Global 'high' resolution model	Uniform 1°x1° latitude-longitude grid. 20 levels in the vertical. In the upper 1000m the levels are the same as in the tropical model. Isopycnal tracer diffusion.	$6x10^7cm^2s^{-1}$
Global 'low' resolution model	Uniform 2.5°x3.75°latitude-longitude grid. 20 levels in the vertical with the same distribution as the 'high' resolution model. Isopycnal tracer diffusion.	$3x10^9cm^2s^{-1}$

TABLE 1: Model Details

In all three model simulations the temperature and salinity fields were initialised from the Levitus (1982) climatology using the monthly mean for September and the currents were initialised to zero.

The wind stress, heat flux and fresh water flux forcing was taken from a long integration of the Hadley Centre atmospheric GCM with seasonally varying climatological sea surface temperatures (see Murphy, 1995 for details). The surface forcing fluxes as calculated by the atmospheric model are known to be generally within the uncertainty of the observed estimates of these quantities (Gordon, 1989, Gordon and Wright, 1995). For the heat and fresh water flux a Haney type (Haney, 1971) surface flux condition was used, so that, for the case

of the surface heating, the total surface flux (the penetrative solar is treated independently and absorbed below the ocean surface) Q is given by:

$$Q(T) = Q(T_c) + \lambda(T_c - T) \quad (2)$$

where T_C is the climatological sea surface temperature (SST) and T the model predicted SST. $Q(T_C)$ is the heat flux with climatological SST and is therefore the heat flux produced by the atmospheric model. Although not the usual form for Haney forcing, the expression (1) is exactly equivalent to the usual formulation in terms of an effective air temperature. The coefficient λ was set equal to $163 Wm^{-2}K^{-1}$ in all the model versions. For a 100m layer of water, this is equivalent to a relaxation time of approximately one month. This large value of λ was chosen to ensure that the predicted SSTs do not drift too far from climatology and also to be consistent with the climate change experiments with the coarse model carried out by Murphy (1995). The Haney term is necessary to prevent the simulated SST drifting too far from the observed climatology. In a fully coupled atmosphere-ocean model the air-sea interactions provide the appropriate feedback on the SST although flux correction may still be necessary to prevent climate drift (see e.g. Murphy, 1995). Such a strong forcing back to climatology does mean, however, that there is little to be learnt by comparing the SSTs from each of the model simulations.

Each model integration was for four years, by which time the tropical oceans have effectively reached equilibrium in the sense that the mean features in year four are essentially the same as those in year three. The results shown in the next section for the annual mean state are from year four of each model simulation.

3. The Simulation of Mean Features

The richness of ocean current structure in the tropical Pacific is now well documented and the main features are shown clearly in the now classic figures of Wyrtki and Kilonsky (1984), which are reproduced in fig.1. Fig.1a shows the derived annual mean current structures from the Hawaii-to-Tahiti shuttle data. The SEC, NEC, EUC and NECC can all clearly be seen. The EUC has a maximum speed of 90 cms^{-1} and the NECC a maximum speed of 40 cms^{-1}. The region above the under-current and below the SEC contains strong non-

linear interactions leading to a local minimum of surface zonal velocity on the equator. The NECC maximum is below the surface because in the near surface layers there is a cancellation between the geostrophic eastward sub-surface current and the near surface wind driven flow.

The corresponding temperature field from the Shuttle data is shown in fig.1b. The spreading of the thermocline associated with the undercurrent is evident as is the 'dipping' and 'doming' which gives rise to the counter-current. Much of this meridional thermocline structure can simply be understood in terms of the vertical velocity field caused by Ekman pumping. The wind field on the equator has a typical easterly component of 0.2 - 0.5 dyne/cm^2, moving northwards this decreases to near zero in the region of the Inter-Tropical Convergence Zone (ITCZ) and then increases again into the centre of the North East Trades where there are stresses of over 1 dyne/cm^2. Simple Ekman pumping gives the vertical velocities proportional to curl($\underline{\tau}$/f), which effectively reduces to:

$$-\frac{\partial}{\partial y}(\tau_x / f) = -\frac{1}{\beta y}\frac{\partial \tau_x}{\partial y} + \frac{\tau_x}{\beta y^2} \qquad (3)$$

where the equatorial β-plane approximation f=βy, and the fact that $|\tau_X| >> |\tau_Y|$, has been used. Clearly expression (2) is invalid very close to the equator (within an equatorial Rossby radius) where Ekman pumping does not apply. For small y (but larger than the Rossby radius) the second term dominates, so that the convergence occurring because the Coriolis parameter increases rapidly away from the equator produces downwelling, leading to the 'dipping' of the thermocline around 5°N. The reduction in τ_X from the equator to the ITCZ also produces a convergence and downwelling. Between the ITCZ and the NE Trades, the first term in (2) is positive (because τ_X gets larger in a negative sense) and this induces upwelling that causes the 'doming' of the thermocline that is evident in fig.1b around 10°N.

The simulation of these tropical features in the models with different horizontal resolution are shown in figs.2 and 3. Figs.2a, 2b and 2c show the annual mean simulated current structure through 155°W from the tropical Pacific, the global one degree and the coarse global models respectively. These should be compared with the currents derived from the Shuttle data shown in fig.1a.

The tropical Pacific model captures the major features in the equatorial currents. The undercurrent has a peak speed of 70cms^{-1} compared to 90cms^{-1} from the Shuttle data. This is well within the uncertainty that can be expected because of inaccuracies in the wind stress forcing (Gordon and Corry, 1991). The counter-current has a peak speed of 50cms^{-1}, which is slightly larger than the Shuttle data and is again probably a consequence of the wind forcing used. The speed of the countercurrent is particularly sensitive to the wind stress curl associated with the ITCZ region, as explained earlier in relation to the meridional thermocline structure. The major shortcoming in the simulation is the spreading of the under-current below the core to a depth of more than 350m, whereas in the data the zero current occurs near to 250m. This could be due to the vertical mixing scheme used or, in part, to the relatively coarse vertical resolution at these depths.

The simulated currents using the one degree global model are shown in fig.2b. The peak undercurrent speed is now 60ms^{-1} and the counter-current speed 40cms^{-1}. These slower current speeds, compared to the higher resolution tropical model, are to be expected both from smoothing by the coarser grid and also by the higher eddy viscosity coefficient (see table 1). Although there are significant differences between this simulation and that produced by the tropical Pacific model as shown in fig.2a, all of the major features are captured by the global 1°x1° model. It is interesting that this model does not extend the under-current as deep as the tropical Pacific model.

The simulation of the tropical Pacific currents using the coarser resolution 2.5° x3.75° model is shown in fig.2c. The currents here are very different to the previous two models. Most of the major features are not captured. There is a token undercurrent of 10cms^{-1} and no countercurrent. The surface flow has more of a simple Yoshida jet like structure (Gill, 1982), indicating the lack of vertical momentum transfers which were evident in the previous two models. With a meridional resolution of 2.5° and a horizontal eddy viscosity a factor of 100 larger than in the tropical Pacific model, it is not surprising that the simulation is so poor.

The north-south vertical temperature cross-sections associated with the above current structure are shown if figs.3a, b and c. These should be compared to the observed Shuttle temperature cross-section in fig.1b. For both the tropical Pacific model and the one degree model the temperature cross-sections show all

the major features present in the data. In particular they show the spreading associated with the undercurrent and the dipping and doming associated with the counter-current. As can be anticipated from the current simulation, the coarser 2.5°x3.75° model does not capture the meridional variations in thermal structure and produces a poor simulation of these features.

In terms of the mean climate simulation in a coupled model the inability of the coarse resolution ocean to properly represent the mean tropical dynamics may not be of great significance. When considering the transient features, however, in may well be very important (next section). The lack of an undercurrent in the coarse resolution model can effect the mean heat budget in the east Pacific where the undercurrent surfaces and thereby effects the mixed layer temperatures. The lack of a counter-current can also lead to an incorrect simulation of SST under the ITCZ and therefore affect the deep convective forcing in the atmospheric component of the coupled model. In fact, the positioning of the ITCZ is determined by coupled processes. The ITCZ is above the warmest water which stretches across the Pacific (see fig.3) and is associated with the NECC. The positioning of the NECC is, in turn, determined by the wind-curl forcing as previously described. Finally, the wind forcing is determined by the detailed positioning of the convergence zone. The higher resolution ocean models are able to capture the major features involved in the ocean component of this coupled loop whereas the coarse model cannot.

4. The Simulation of Transient Features

Although the simulation of the mean features in models of different resolution is of interest, it is the Kelvin and Rossby waves that are of primary importance when considering the transient behaviour of particular relevance to El Nino. In this section some simple wind burst experiments are described and the wave propagation from these bursts illustrated for the 1°x1° and 2.5°x3.75° models. The mean results of the previous section suggest that the transient features in the tropical model (at least for the first few modes) will be similar in character to those in the global 1°x1° simulation.

The behaviour of Kelvin waves in models of different meridional resolution has recently been investigated by Ng and Hsieh (1994). Fig.4 is reproduced from their paper and shows the theoretical dependence of the phase speed of the

Kelvin wave, expressed as a fraction of the analytical value, on the meridional grid spacing scaled with the Rossby radius. This curve is appropriate to a finite difference B-grid with a tracer point on the equator (as used in the Cox model).

In the GCM simulations the dominant mode has a phase speed of approximately $2.7ms^{-1}$ in the 1°x1° model (see later) which then implies a Rossby radius of 240km for this mode. With reference to fig.4 this then gives $\Delta=0.86$ (where Δ is the grid spacing in units of the Rossby radius) for the 2.5° x3.75° model and $\Delta=0.46$ for the 1°x1° model. The theoretical ratio of the Kelvin wave phase speeds can be read off from fig.4 to be $C_{2.5x3.75}/C_{1x1}=0.97$ and so the phase speed is only slightly reduced by the direct effect of the coarser resolution. For higher modes the phase speed decreases, as does the Rossby radius, and the values of Δ will therefore increase. This means that higher modes are progressively slowed down more by the increasing grid size. For a detailed simulation of the physics of ENSO, which means resolving these higher modes, it is therefore necessary to retain the high meridional resolution used in the tropical model.

To investigate the propagation of Kelvin and Rossby waves in the 1°x1° and 2.5°x3.75° models further, some simple wind burst experiments were carried out. The wind bursts were applied from the same starting time in each of the models. Climatological seasonal forcing was used as the background forcing in each case. In the first experiment the burst had a maximum speed of $5ms^{-1}$ and a duration of 10 days, including a ramping in and out. The burst was located west of the dateline between 150°W and 180°W. The wind burst used was identical to that used by Davey (1992) in his experiments and details of its implementation can be found in this paper. Fig.5, which has been reproduced from Davey (1992), shows the spatial and time structure of the wind burst.

The actual model responses to the implied wind burst are shown in the equatorial time-longitude plots in fig.6. Fig.6a and 6b show the eastward component of the current difference averaged over the top 113m of each model, calculated by subtracting the eastward current obtained with the use of mean seasonal forcing from the eastward current obtained with the addition of the wind anomaly. For both models these plots are for the currents averaged over grid points within the latitude range 4°S to 4°N. As expected from the results of Ng and Hsieh the phase speed of the wave is slightly slower in the 2.5°x3.75° model.

Comparison of figs.6a and 6b shows many differences. The phase speed of the dominant Kelvin wave in fig.6a is 2.7ms^{-1} and it maintains a strong amplitude all the way to the eastern boundary. For the second most dominant Kelvin mode evident in the 1°x1° model simulation, the phase speed is 1.4ms^{-1} whereas there is no evidence of this mode in the 2.5°x3.75° windburst experiment. The theory of Ng and Hsieh would suggest a phase speed of 1.2ms^{-1} if such a mode were present in the low resolution model.

In the 1°x1° simulation there is also clear evidence of Rossby wave reflection at the eastern boundary which then interferes with the second incoming Kelvin mode. In the coarse model there is no significant Rossby reflection as the Kelvin mode has essentially dissipated by the time it reaches the eastern boundary. A curious feature in the one degree model is the lack of Kelvin wave reflection at the western boundary arising from the initial Rossby mode from the wind burst (fig.6a). The reasons for this are unclear and may be associated with the open western boundary in the global 1°x1° model. In simple simulations with a shallow water equation model, lack of reflection can occur due to the detailed shape of the model western boundary which can lead to destructive interference of the reflected waves (M.K. Davey, private communication). This needs further investigation.

The wind burst in the experiments described above had a duration of only 10 days. During ENSO there are interannual changes in the equatorial winds of much longer duration, typically of several months to a year. As indicated in the 10 day wind burst experiment the 1°x1° model is well capable of simulating at least the first few modes associated with longer term ENSO type wind anomalies. It is, however, also relevant to assess the response of the 2.5°x3.75° model to a much longer ENSO-type forcing. An experiment was performed with the 2.5°x3.75° model in which the wind anomaly had the same shape as used above but with a spatial positioning and time profile more typical of ENSO-like wind anomalies. The spatial shape is still that represented in fig.5a but now shifted to the east so that the wind burst in contained between the dateline and 150°W (rather than 150°E to the dateline as before). The time profile was the same shape as shown in fig.5b but with the time axis in weeks rather than days, that is, the anomaly was ramped in over a two week period, maintained at 5ms^{-1} for six weeks and then ramped out over a further two week period.

The modelled anomalous equatorial eastward current in response to this wind anomaly is shown in fig.7. Once again there is a large local response to the wind anomaly but a very rapid decay of the Kelvin and Rossby wave signal away from the forcing region. Once the forcing is switched off after 70 days the signal very quickly dissipates.

This experiment confirms that even when subjected to sustained climate time scale wind anomalies the 2.5°x3.75° model only produces a significant local response with the non-local response being heavily damped.

These results can be summarised as follows:

1°x1° Model	This model shows a clear Kelvin wave signal that propagates into the east Pacific and reflects at the eastern boundary into a Rossby mode. Higher Kelvin modes are also present.
2.5°x3.75° Model	The dominant Kelvin mode is highly damped in this model as it propagates away from the source region and only reaches the eastern boundary with very low amplitude. There is no evidence of significant reflected Rossby modes or higher Kelvin modes.

5. ENSO Mechanisms

A number of different mechanisms have been suggested for the generation of the ENSO cycle in the coupled tropical system. McCreary and Anderson (1991) identify three major mechanisms which they characterise as: a) the delayed oscillator mechanism, b) the existence of two equilibrium states (which is a special case of (a)), and c) the existence of coupled instabilities. Mechanism (a) crucially relies upon the slow propagation of ocean Rossby waves to set the timescale and the reflection of these at the western boundary into Kelvin waves to 'close' the oscillator. From the results in the previous sections these modes will not be well represented in the coarser resolution models (such as the 2.5°x3.75° model) in which the free ocean waves are heavily damped.

The third mechanism, associated with coupled instabilities, is somewhat different. The coupled modes depend upon the local coupling of the oceanic and atmospheric response either explicitly in terms of waves (McCreary and Anderson, 1991) or arising from local couplings associated with air-sea interactions independent of ocean wave propagation (Neelin, 1991). In either case, the thermocline disturbance away from the source region is not of primary importance and so modes of this kind are likely to be present in all models irrespective of the resolution (and the implied damping of the free ocean waves). Essentially the forcing of the ocean part of these modes is local and moves with the mode so that free propagating ocean waves do not play an important part.

6. Conclusions

The main purpose of this paper has been to quantify the effect of model latitudinal resolution on the simulation of mean and transient tropical ocean dynamics. The result that the coarser resolution model does particularly poorly is of no surprise considering the 2.5° latitudinal resolution compared to the Rossby radius and the large eddy viscosity that has to be used in the model to maintain numerical stability. The one degree model does appear to be able to capture the major features of the tropical dynamics although this resolution is still 'coarse' when considering higher modes which will be damped more heavily than those considered above.

For ENSO simulation the results in this note make plain that the coarser resolution models are able to simulate the basic physics of the local coupled SST modes but are not able to represent those modes that depend upon freely propagating ocean waves. For detailed ENSO studies these results point to the continued need for models with a high meridional resolution in the tropics. For longer term climate oriented studies, where long integration times are necessary, a resolution of one degree has been shown to provide a considerably more realistic simulation of the tropical dynamics than the coarser 2.5°x3.75° model.

A number of future studies are suggested by the simple numerical experiments described above. In terms of the simulation of mean features a comparison of

the positioning and seasonal variations within the ITCZ/NECC system in high and low resolution coupled models would be of value. In terms of the transient behaviour the reflection of Rossby waves at the western boundary is crucial to a number of proposed ENSO cycle mechanisms and this does not appear to be represented in the models. In this regard, further studies at high resolution with an open and closed western boundary (i.e. with and without flow through to the Indian Ocean) would be useful.

Acknowledgements

We would like to thank Dr M.K. Davey and Dr H. Cattle for their helpful comments on a draft version of this paper. This work was partially supported under CEC contract EV5V-CT92-0121, Medium Term Climate Variability.

REFERENCES

Cox, M.D. (1984) A primitive equation 3 dimensional model of the ocean. GDFL Ocean Group Technical, Report No 1.

Davey, M.K. (1992) A tropical ocean model with reduced physics. Climate Research Technical Note No. 29, Hadley Centre, UK Meteorological Office.

Gill, A.E. (1982) Atmosphere-Ocean Dynamics. Academic Press.

Gordon, C. (1989) Tropical Ocean-Atmosphere Interactions in a coupled model. Phil. Trans. R. Soc. A 329,207-223.

Gordon, C. (1989) Comparison of the surface fluxes in the tropical Pacific ocean derived from an atmospheric GCM and from climatology. Tropical Ocean-Atmosphere Newsletter, No. 51.

Gordon, C. and Corry, R.A. (1991) An ocean model simulation of the seasonal cycle in the tropical Pacific ocean using climatological and modelled surface forcing. J. Geophy. Res. 96, No.C1, 847-864.

Gordon, C. and D. K. Wright (1995) A comparison of modelled surface fluxes with climatological estimates. Climate Research Technical Note No.53, Hadley Centre, UK Meteorological Office.

Haney, R.L. (1971) Surface thermal boundary conditions for ocean circulation models. J. Phys. Oceanogr. 1, 241-248.

Knutson, T.R. and S. Manabe (1994) Impact of increased CO_2 on simulated ENSO-like phenomena. Geophys. Res. Letts. 21, No.21, 2295-2298.

Levitus, S. (1982) Climatological Atlas of the World Ocean, NOAA Professional Paper 13.

McCreary, J.P. and D.L.T. Anderson (1991) An overview of coupled ocean-atmosphere models of El Nino and the Southern Oscillation. J. Geophys. Res., 96, 3125-3150.

Mechoso, C.R., A.W. Robertson, N. Barth, M.K. Davey, P. Delecluse, P.R. Gent, S. Ineson, B. Kirtman, M. Latif, H. Le Treut, T. Nagai, J.D. Neelin, S.G.H. Philander, J. Polcher, P.S. Schopf, T. Stockdale, M.J. Suarez, L. Terray, O. Thual, J.J. Tribbia (1995) The seasonal cycle over the tropical Pacific in general circulation models. (Submitted to Monthly Weather Review.)

Meehl, G.A., G.W. Branstator and W.M. Washington (1993) Tropical Pacific interannual variability and CO_2 climate change. J. Clim.,6,42-63.

Murphy, J.M. (1995) Transient response of the Hadley Centre coupled ocean-atmosphere model to increasing carbon dioxide. Part I: Control climate and flux adjustment. J. Clim., 8, 36-56.

Neelin, J.D. (1991) The slow SST mode and the fast-wave limit: Analytic theory for tropical interannual oscillations and experiments in a hybrid coupled model. J. Atmos. Sci., 48, 584-606.

Ng, M.K.F. and W.W. Hsieh (1994) The equatorial Kelvin wave in finite-difference models. J. Geophys. Res., 99, 14,173-14,185.

Philander, S.G.H., N.C. Lau, R.C. Pacanowski and M.J. Nath (1989) Two different simulations of the Southern Oscillation and El Nino with coupled ocean-atmosphere general circulation models. Phil. Trans. R. Soc. Lond. A 329, 167-178.

Redi, M.H. (1982) Oceanic isopycnal mixing by coordinate rotation. J. Phys. Oceanogr. 12, 1154-1158.

Tett, S. (1995) Simulation of El-Nino/Southern Oscillation like variability in a global AOGCM and its response to CO_2 increase. J. Clim. (to appear).

Wyrtki, K. and B. Kilonsky (1984) Mean water and current structure during the Hawaii-to-Tahiti shuttle experiment. J. Phys. Oceanog., 14, 242-253.

FIGURE CAPTIONS

Fig.1: Cross sections of zonal velocity (1a) in cms^{-1} and the temperature (1b) between Hawaii and Tahiti (roughly 155°W) as measured during the Hawaii-to-Tahiti shuttle experiment. (From: Wyrtki and Kilonsky, 1984).

Fig.2: Cross sections of zonal velocity (cms^{-1}) along 155°W from a) the high resolution tropical model, b) the 1°x1° global model and c) the 2.5°x3.75° global model.

Fig.3: Cross sections of temperature along 155°W from a) the high resolution tropical model, b) the 1°x1° global model and c) the 2.5°x3.75° global model.

Fig.4: The dependence of Kelvin wave phase speed (expressed as a fraction of the analytic value) as a function of grid spacing (expressed as a fraction of the Rossby radius) on an Arakawa B-grid with a tracer point on the equator. (From: Ng and Hsieh, 1994).

Fig.5: The spatial and temporal structure of the westerly wind burst. (From: Davey, 1992).

Fig.6: The average equatorial current anomaly over the top 113m as a function of time in response to the westerly wind burst. In both models the current is averaged over grid points within 4°N to 4°S. Fig.6a shows results from the one degree model with a contour interval of $5cms^{-1}$ and fig.6b shows results from the 2.5°x3.75° model with a contour interval of $1cms^{-1}$.

Fig.7: The 2.5°x3.75° model average equatorial current anomaly over the top 113m as a function of time in response to the 'ENSO type' westerly wind anomaly. The contour interval is $5cms^{-1}$.

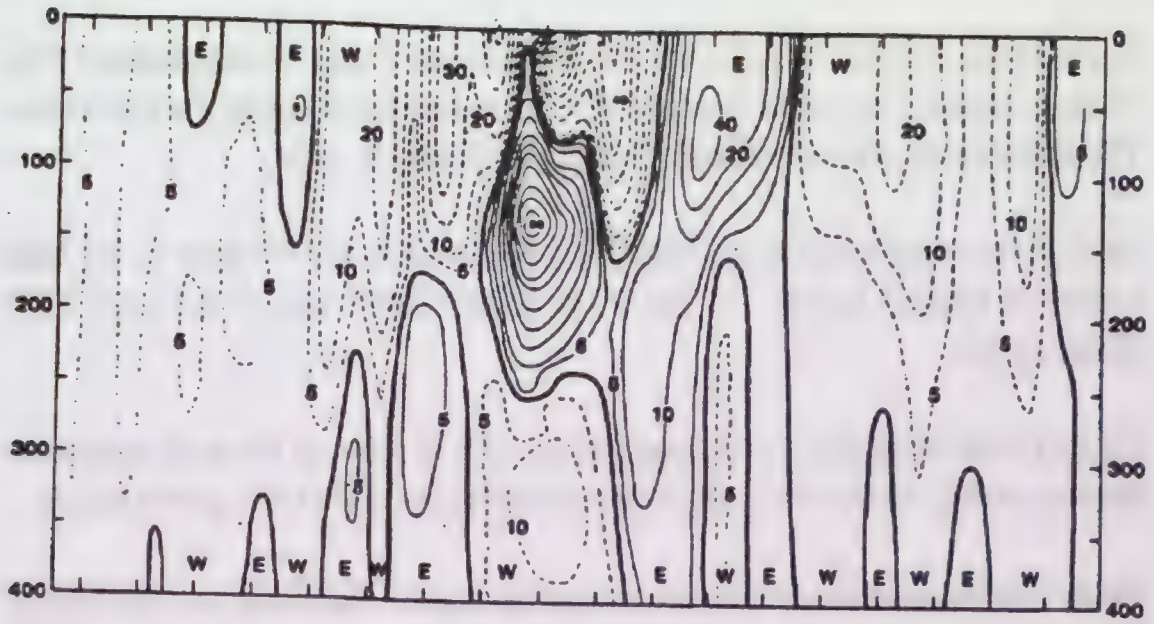
0
100
200
300
400
E
W
5
10
20
30
40

FIG.1a

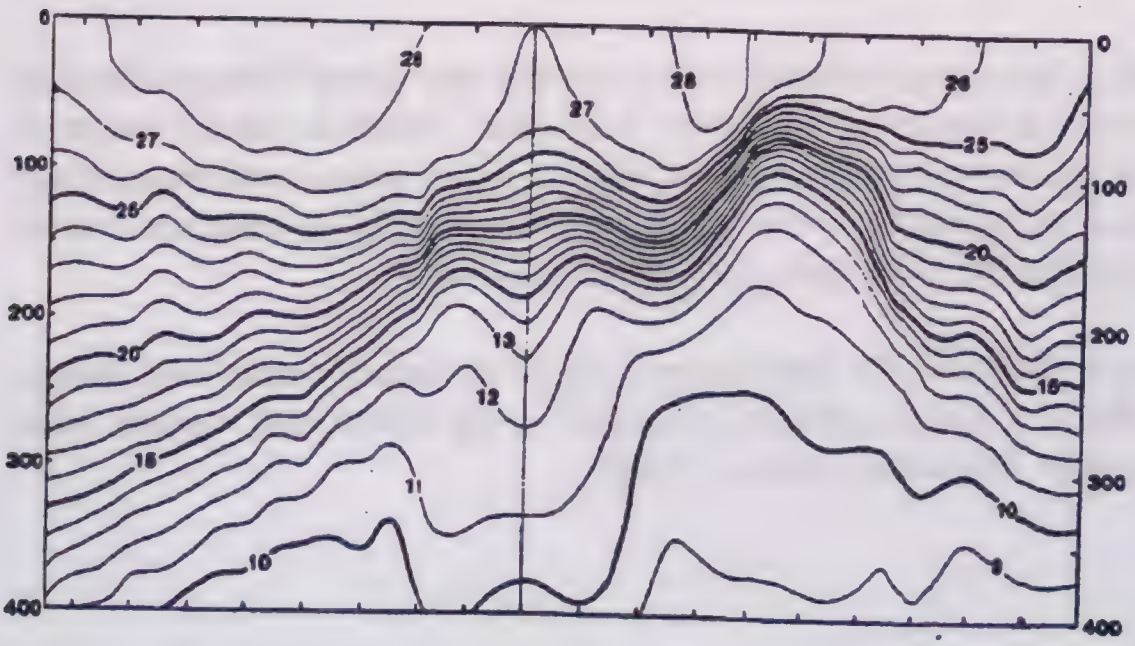
0
100
200
300
400
28
27
26
25
20
15
13
12
11
10
9

FIG.1b

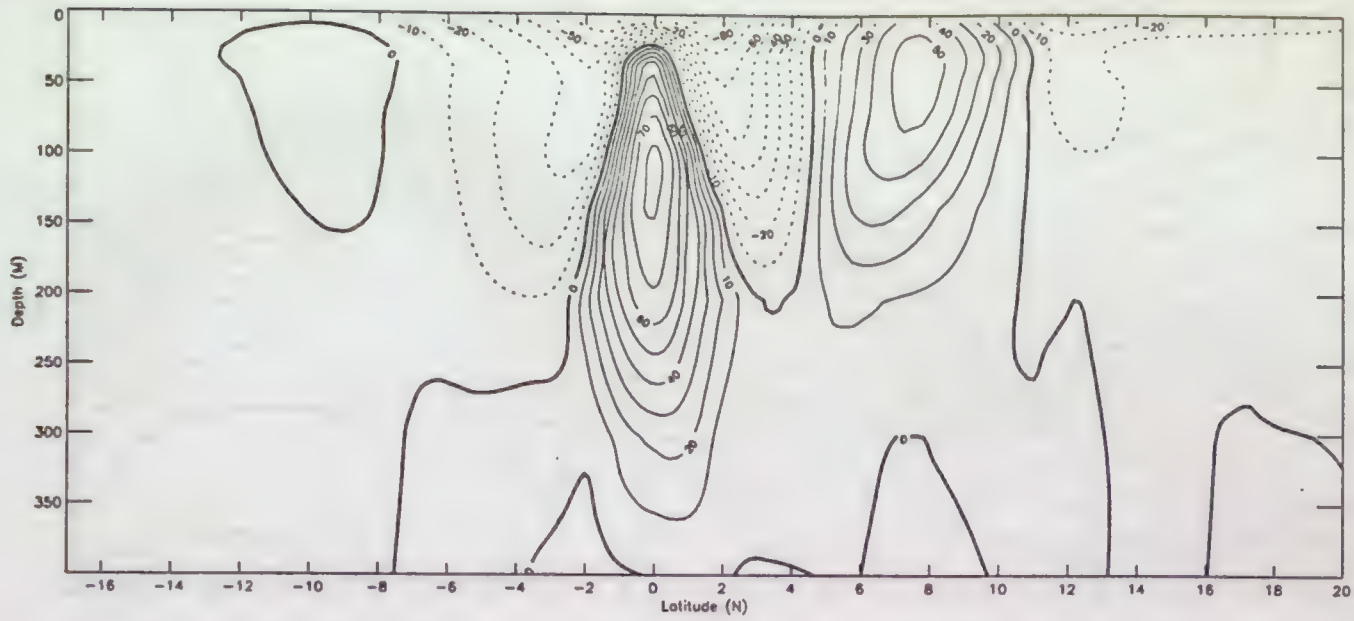

Fig 2a

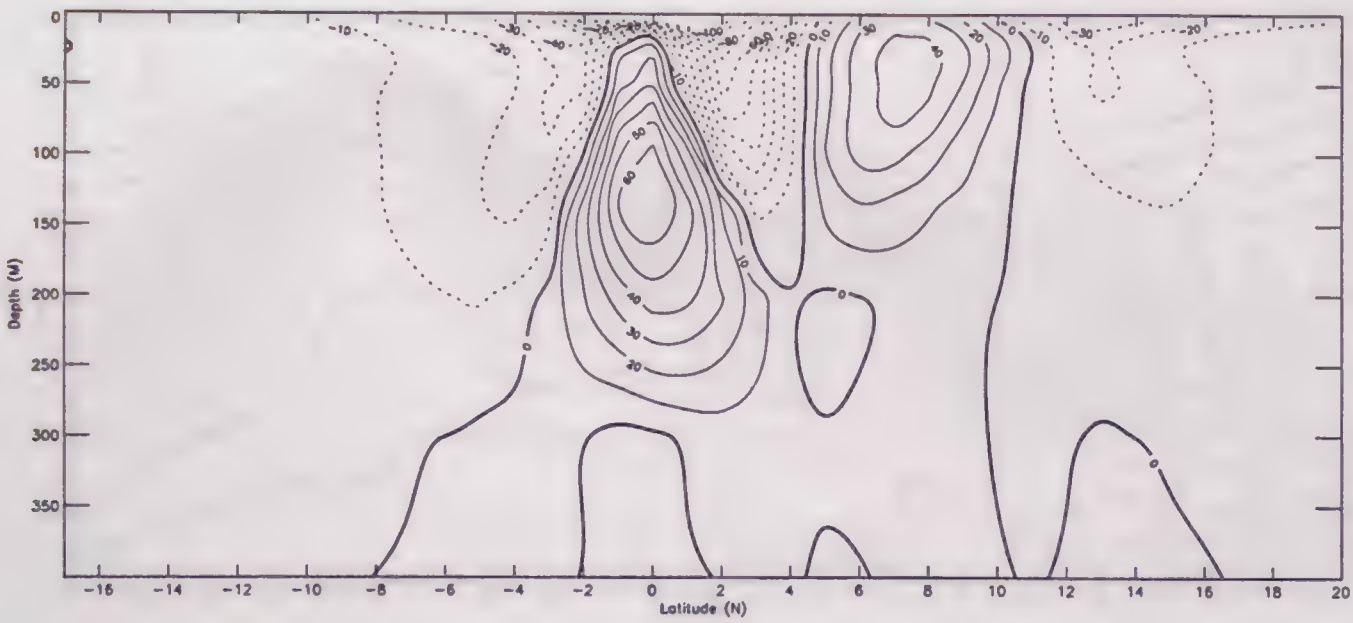

Fig 2b

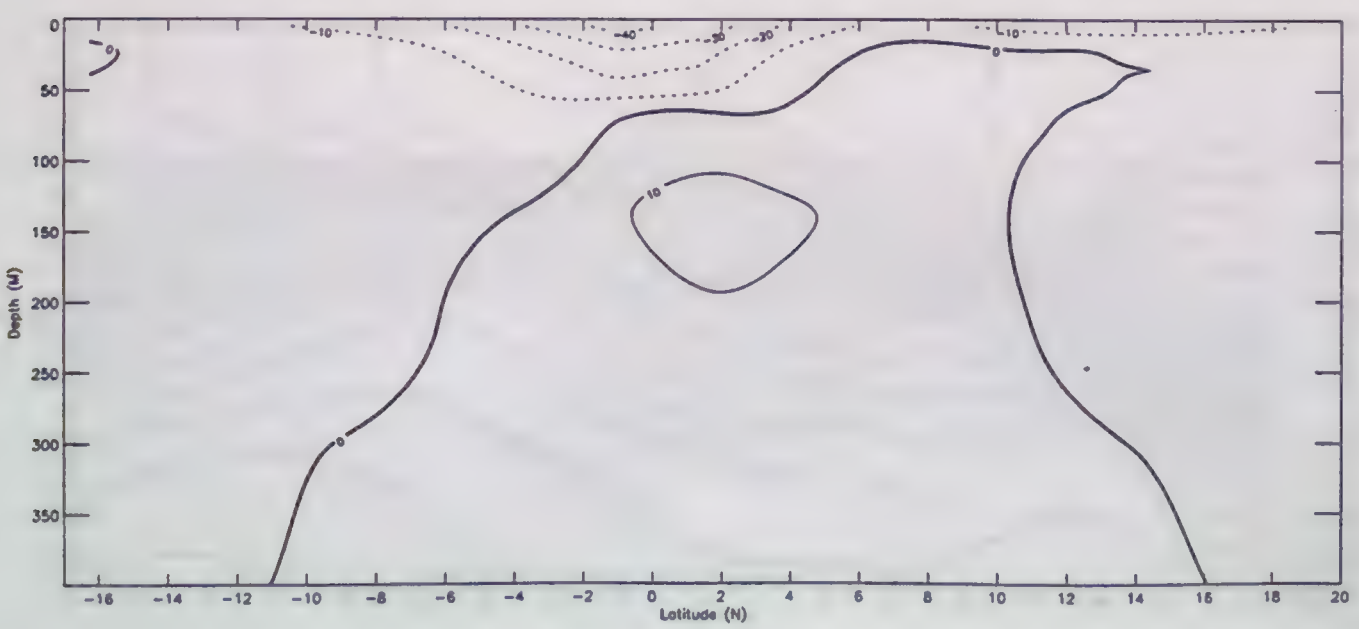

Fig 2c

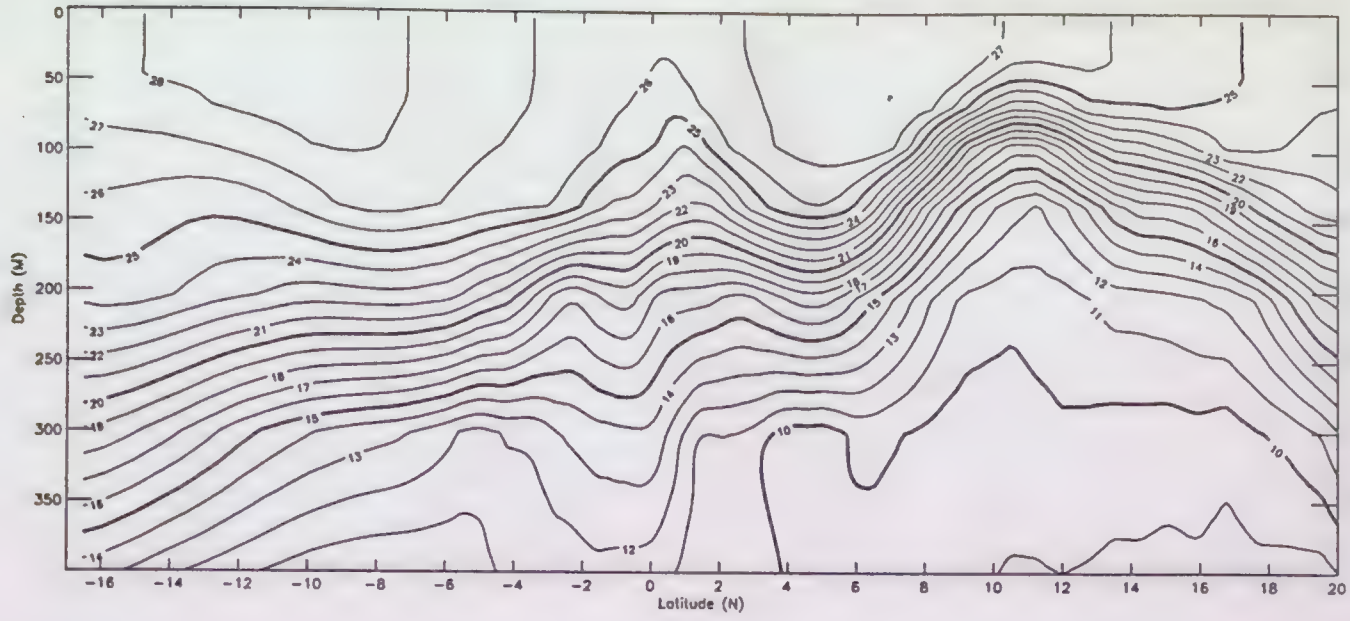

Fig 3a

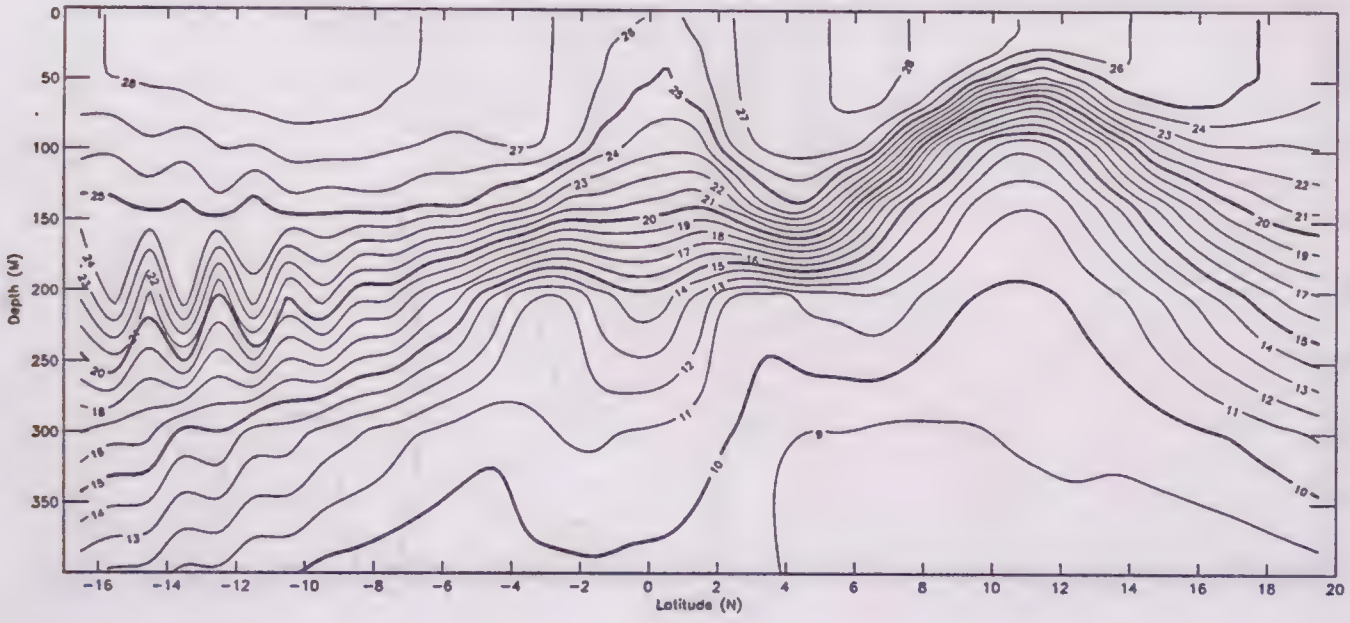

Fig 3b

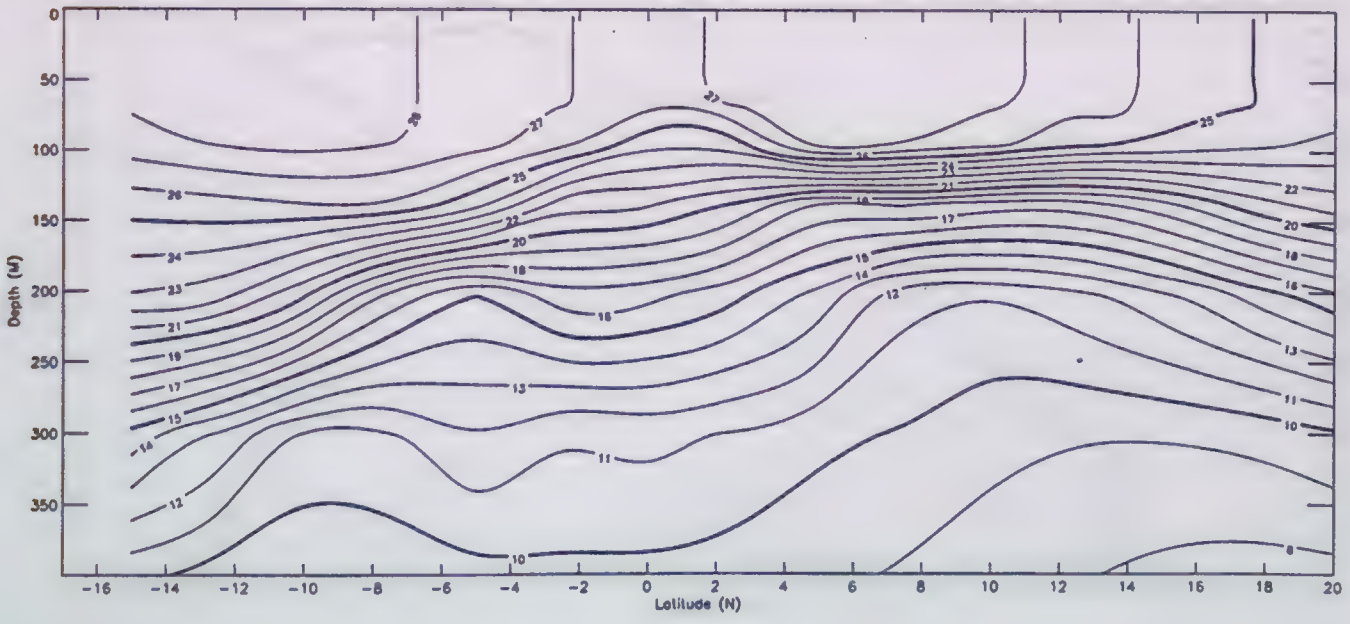

Fig 3c

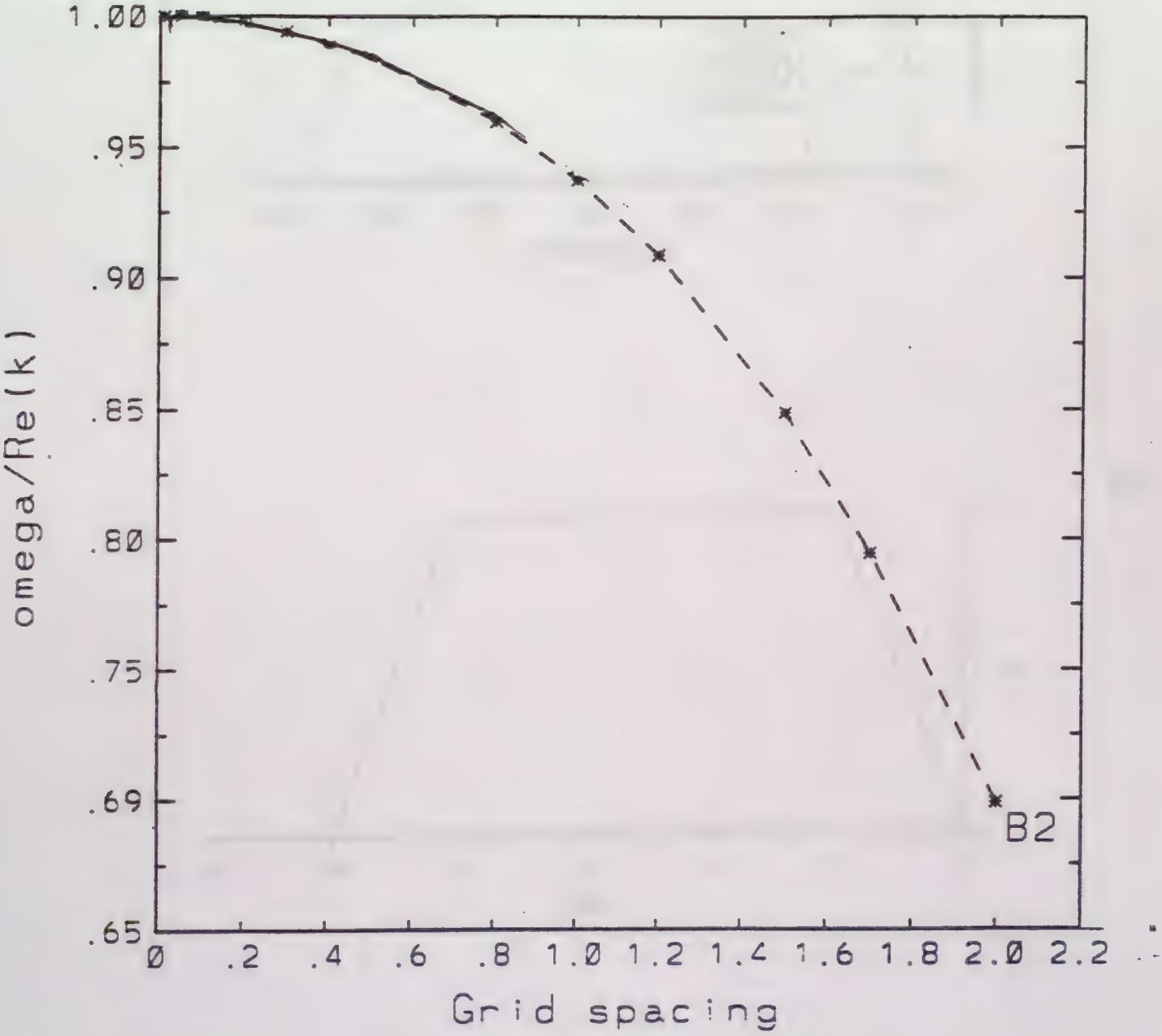
1.00
.95
.90
.85
.80
.75
.69
.65
omega/Re(k)
0
.2
.4
.6
.8
1.0
1.2
1.4
1.6
1.8
2.0
2.2
Grid spacing
B2

FIG.4

(a)

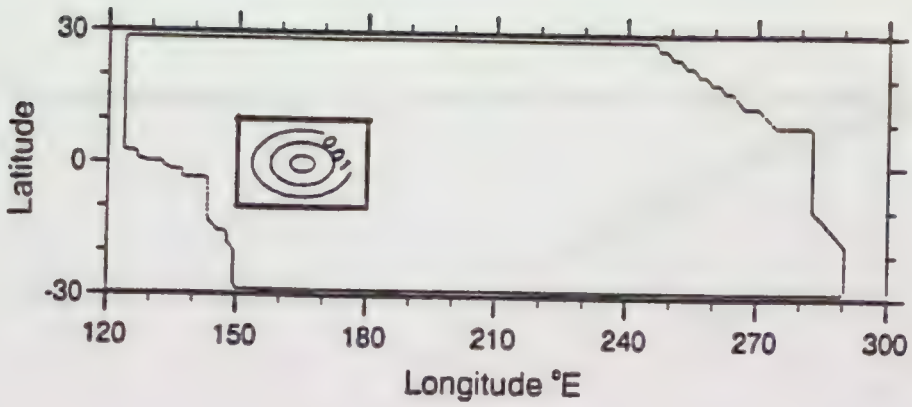

(b)

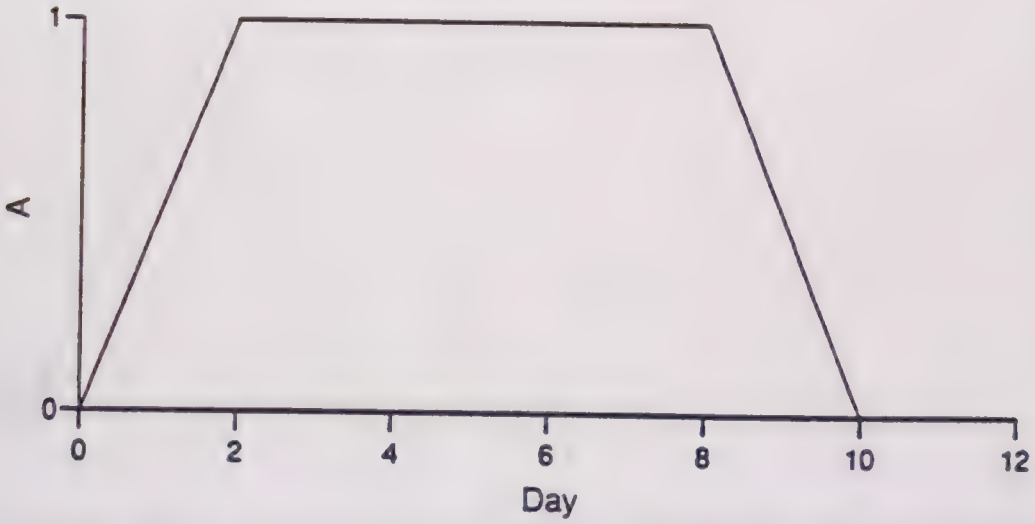

Fig. 5 Structure of the westerly windburst.

(a) The zonal wind stress at day 5.
Max = 0.032 $N\ m^{-2}$

(b) Time profile of amplitude A(t).

FIG.6a

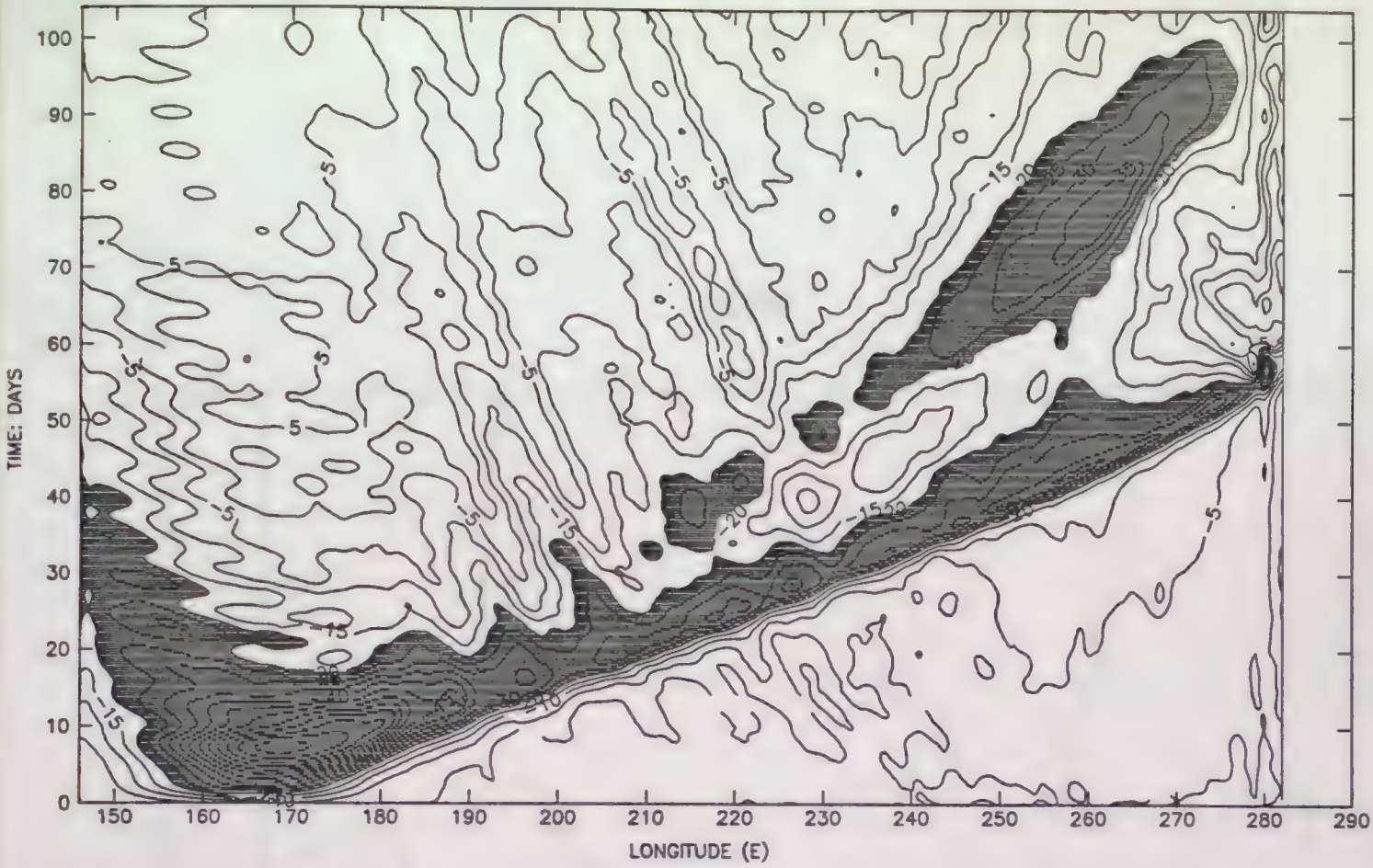
TIME: DAYS
LONGITUDE (E)
0
10
20
30
40
50
60
70
80
90
100
150
160
170
180
190
200
210
220
230
240
250
260
270
280
290

FIG.6b

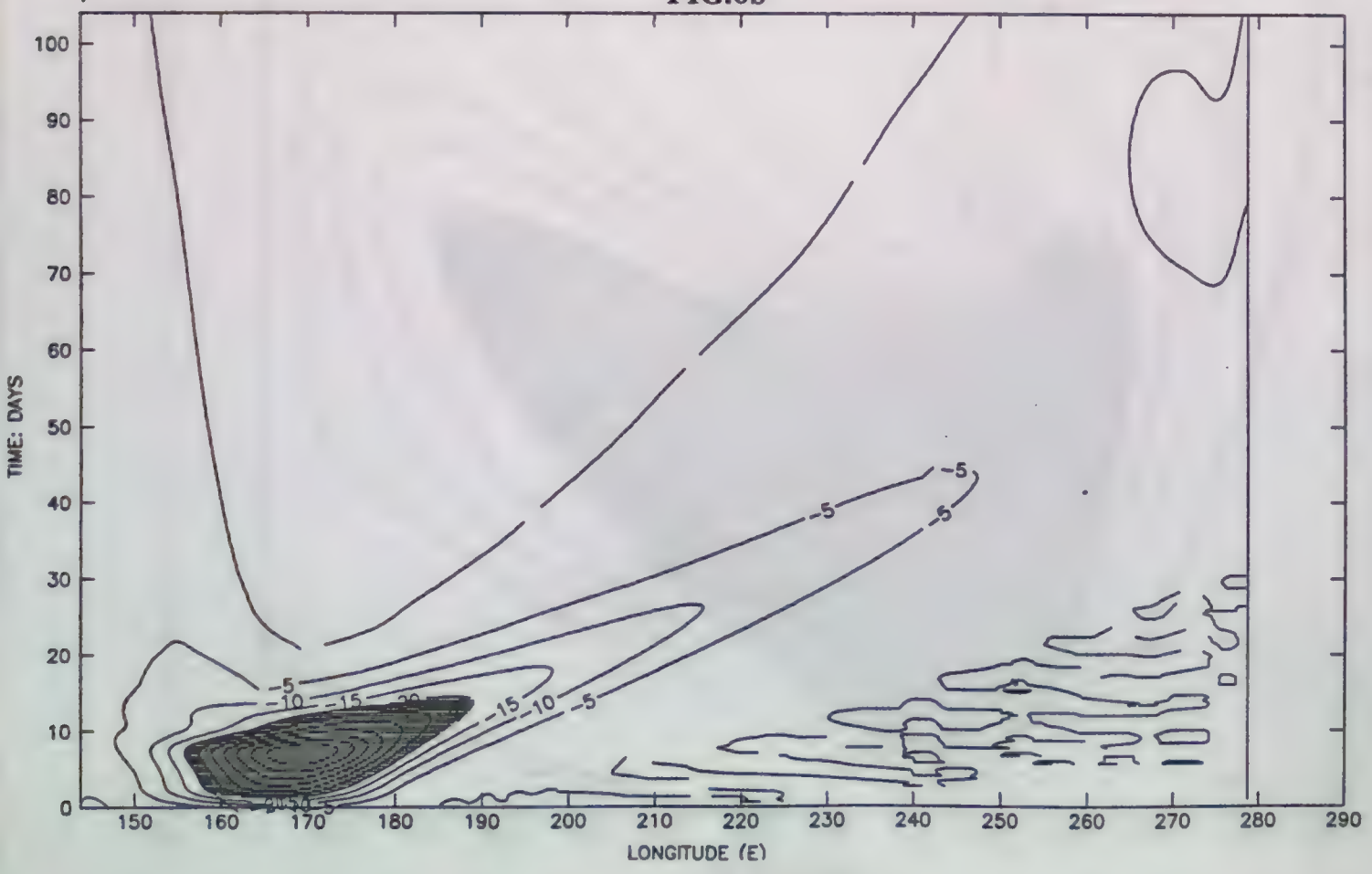
TIME: DAYS
LONGITUDE (E)
0
10
20
30
40
50
60
70
80
90
100
150
160
170
180
190
200
210
220
230
240
250
260
270
280
290

FIG.7

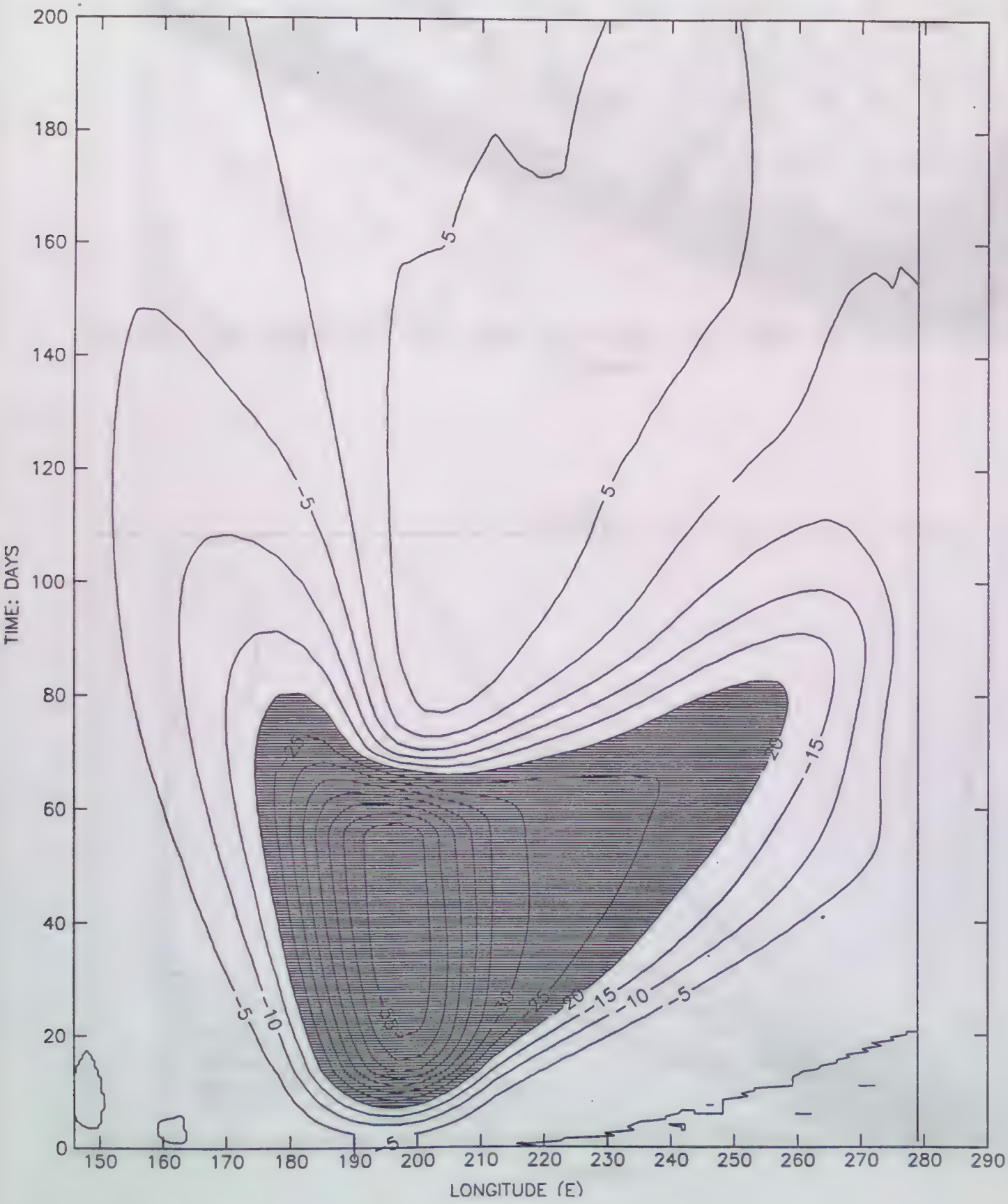
TIME: DAYS
LONGITUDE (E)
200
180
160
140
120
100
80
60
40
20
0
150
160
170
180
190
200
210
220
230
240
250
260
270
280
290
5
-5
-10
-15
-20
-25
-30

CLIMATE RESEARCH TECHNICAL NOTES

CRTN 1	Oct 1990	Estimates of the sensitivity of climate to vegetation changes using the Penman-Monteith equation. P R Rowntree
CRTN 2	Oct 1990	An ocean general circulation model of the Indian Ocean for hindcasting studies. D J Carrington
CRTN 3	Oct 1990	Simulation of the tropical diurnal cycle in a climate model. D P Rowell
CRTN 4	Oct 1990	Low frequency variability of the oceans. C K Folland, A Colman, D E Parker and A Bevan
CRTN 5	Dec 1990	A comparison of 11-level General Circulation Model Simulations with observations in the East Sahel. K Maskell
CRTN 6	Dec 1990	Climate Change Prediction. J F B Mitchell and Qing-cun Zeng
CRTN 7	Jan 1991	Deforestation of Amazonia - modelling the effects of albedo change. M F Mylne and P R Rowntree
CRTN 8	Jan 1991	The role of observations in climate prediction and research. D J Carson
CRTN 9	Mar 1991	The greenhouse effect and its likely consequences for climate change. D J Carson
CRTN 10	Apr 1991	Use of wind stresses from operational N.W.P. models to force an O.G.C.M. of the Indian Ocean. D J Carrington
CRTN 11	Jun 1991	A new daily Central England Temperature series, 1772-1991. D E Parker, T P Legg and C K Folland
CRTN 12	Jul 1991	Causes and predictability of Sahel rainfall variability. D P Rowell, C K Folland, K Maskell, J A Owen, M N Ward

CLIMATE RESEARCH TECHNICAL NOTES

CRTN 13	Jul 1991	Modelling changes in climate due to enhanced CO2, the role of atmospheric dynamics, cloud and moisture. C A Senior, J F B Mitchell, H Le Treut and Z-X Li
CRTN 14	Sep 1991	Sea temperature bucket models used to correct historical SST data in the Meteorological Office. C K Folland
CRTN 15	Aug 1991	Modelling climate change, and some potential effects on agriculture in the U.K. P R Rowntree, B A Callander and J Cochrane
CRTN 16	Aug 1991	The Boreal Forests and Climate G Thomas and P R Rowntree
CRTN 17	Aug 1991	Development of a Stratosphere-Troposphere Data Assimilation System. R Swinbank.
CRTN 18	Sep 1991	A study of asynchronous coupling using a simple climate model. M K Davey.
CRTN 19	Sep 1991	The Oceanic Carbon Cycle. N K Taylor
CRTN 20	Nov 1991	Worldwide ocean-atmosphere surface fields in Sahel wet and dry years using provisionally corrected surface wind data. M N Ward
CRTN 21	Dec 1991	Coupled tropical ocean global atmosphere models at the UKMO. M K Davey, C Gordon, S Ineson and S Lawrence
CRTN 22	Dec 1991	Empirical parameterisation of tropical ocean-atmosphere coupling. M Allen, M K Davey, D L T Anderson and P D Killworth
CRTN 23	Feb 1992	The temporal evolution of Equatorial Currents in the Indian Ocean D L T Anderson, D J Carrington, R A Corry and C Gordon
CRTN 24	Feb 1992	Stratospheric analyses provided by the U.K. Meteorological Office M J Bailey, A O'Neill and V D Pope

CLIMATE RESEARCH TECHNICAL NOTES

CRTN 25	Feb 1992	Modelling interannual variability in the Indian Ocean using momentum fluxes from the UKMO and ECMWF operational weather analyses. D L T Anderson and D J Carrington
CRTN 26	Mar 1992	A GCM simulation of the impact of Amazonian deforestation on climate using an improved canopy representation J Lean and P R Rowntree
CRTN 27	Mar 1992	The parameterization of rainfall interception in GCMs A J Dolman and D Gregory
CRTN 28	Jun 1992	Development of worldwide marine data eigenvectors since 1985 A W Colman
CRTN 29	Jun 1992	A tropical ocean model with reduced physics M K Davey
CRTN 30	Jun 1992	International Temperature Workshop, Boulder, Colorado, USA, 16 January 1992 Edited by D E Parker
CRTN 31	Jul 1992	Simulation of clear-sky outgoing longwave radiation over the oceans using operational analyses A Slingo and M J Webb
CRTN 32	Sep 1992	A prediction of the transient response of climate J M Murphy
CRTN 33	Nov 1992	LEPS scores for assessing climate model simulations and long-range forecasts. C K Folland
CRTN 34	Jan 1993	Stratospheric Data Assimilation System Guide Editer: R Swinbank
CRTN 35	Mar 1993	A Stratosphere-Troposphere Data Assimilation System R Swinbank and A O'Neill
CRTN 36	Mar 1993	Validation of hydrological schemes for climate models against catchment data. P R Rowntree and J Lean

CLIMATE RESEARCH TECHNICAL NOTES

CRTN 37	Apr 1993	Modelling of palaeoclimates: Examples from the recent past J F B Mitchell
CRTN 38	May 1993	A simulation of seasonality in ENSO forecast skill M K Davey, D L T Anderson and S Lawrence
CRTN 39	Jul 1993	ENSO Prediction experiments using a simple ocean-atmosphere model D-H Wu, D L T Anderson and M K Davey
CRTN 40	Sep 1993	Diagnosis of dynamic sea-surface and sea-level changes from the Cox ocean model J M Gregory
CRTN 41	Sep 1993	Seasonal variations of the clear-sky greenhouse effect: the role of changes in atmospheric temperatures and humidities M J Webb, A Slingo and G L Stephens
CRTN 42	Nov 1993	Sea-level changes under increasing atmospheric CO_2 in a transient coupled ocean-atmosphere GCM experiment. J M Gregory
CRTN 43	Dec 1993	Global and regional patterns of climate change: recent predictions for the Arctic P R Rowntree
CRTN 44	Feb 1994	The effect of changing horizontal diffusion in the atmospheric version of the unified climate model C D Hall and R A Stratton
CRTN 45	Mar 1994	Simulation of El-Niño/Southern Oscillation like variability in a global AOGCM and its response to CO_2 increase. S F B Tett
CRTN 46	Apr 1994	Global data required for monitoring climate change. D E Parker and C K Folland
CRTN 47	May 1994	Seasonal uptake of anthropogenic CO_2 in an ocean general circulation model. N K Taylor

CLIMATE RESEARCH TECHNICAL NOTES

CRTN 48	Jun 1994	A tropic-wide oscillation of boreal summer rainfall and patterns of sea-surface temperature. M N Ward, K Maskell, C K Folland, D P Rowell and R Washington
CRTN 49	Jun 1994	Simulation of the tropical Pacific using a simplified ocean model M A Balmaseda, D L T Anderson and M K Davey
CRTN 50	Sep 1994	Simulation of global mean temperature using a box-diffusion climate model P R Rowntree
CRTN 51	Sep 1994	Seasonal dependence of ENSO prediction skill M A Balmaseda, M K Davey and D L T Anderson
CRTN 52	Nov 1994	Simulation of the Indian Monsoon and Tropical Intraseasonal Variability by a General Circulation Model P M Inness and D Gregory
CRTN 53	Mar 1995	A comparison of modelled surface fluxes with climatological estimates. C Gordon and D K Wright
CRTN 54	Mar 1995	The representation of moist convection in atmospheric models. D Gregory
CRTN 55	Mar 1995	A consistent treatment of the evaporation of rain and snow for use in large-scale models D Gregory
CRTN 56	Apr 1995	Workshop on simulations of the Climate of the Twentieth Century using GISST, 28-30 November 1994, Hadley Centre, Bracknell, UK Edited by C K Folland and D P Rowell
CRTN 57	May 1995	Enhanced shortwave cloud radiative forcing due to anthropogenic aerosols. S E Swartz and A Slingo